







Non-contact Robotic Measurement of Jet Engine Components with 3D Optical Scanner and UTT Method

Krzysztof Kurc^(✉) , Andrzej Burghardt , Piotr Gierlak ,
and Dariusz Szybicki 

Rzeszow University of Technology, al. Powstańców Warszawy 12,
35-959 Rzeszów, Poland
{kkurc, andrzejb, pgierlak, dszybicki}@prz.edu.pl

Abstract. This paper presents a method for the robot-assisted geometric inspection of an aircraft engine turbine stator segment, involving two robots. The first robot was an ABB IRB 1600 with an optical 3D scanner. The second robot was an ABB IRB 140, to automatically inspect the stator vanes at 168 points by the application of a UTT method. If the casting geometry tolerances are met, characteristic coordinates of points across the casting are determined for their further use during an alternative robot-assisted vane wall thickness measurement process. The operating principle of the test stand measurement system is presented, with a specific focus on the measurement strategy. The results of the wall thickness measurements performed on stator vanes are presented in the report. The correctness of the solution has been proved with scans and measurements of two turbine rotor guide vane segments of an aircraft engine provided by courtesy of Consolidated Precision Products Poland sp. z o.o.

Keywords: 3D scanning measurement · UTT measurement · Robot Aircraft engine · Geometry inspection · Vane thickness measurement

1 Introduction

The quality control processes for workmanship related to aircraft engines are undertaken at the manufacturing and assembly stages of component production. The significant time required for these processes, sometimes involving repetitive measurements, has prompted their robotization. Measurements, diagnostics, identification and quality control has been considered in many research papers, [1–10], which feature completed or simulated solutions.

Stators are manufactured by precision casting. Low thrust aircraft engines feature monolithic stator castings with a number of vanes, which range from ten to several dozen. The processing conditions for these castings make it difficult to manufacture large stators for large aircraft engines. In this case, a stator is built as an assembly of ten or more segments, each with 3 to 6 vanes. The casting weight is a decisive factor when selecting the stator casting method. To reduce the casting weight requires the use of thin-wall cored castings with a wall thickness of less than 1 mm. Given the

manufacturing difficulties, complexity and technical requirements, these castings are among the most technologically advanced products, and are usually protected (along with their manufacturing technology) as the intellectual property of the manufacturer; hence their manufacturing methods are not widely published. Precision-made polycrystalline castings of the large thin-wall segments for a turbine stator of an aircraft engine are prone to deformation at the casting solidification stage. Hence, 20% of the castings have defects, caused by many factors. The presented robot-assisted geometric inspection of a stator segment was intended as preliminary geometric verification of the casting by comparison with a CAD model (master). The geometric verification process also identified characteristic coordinates for points on the casting for their further use during a robot-assisted vane wall thickness measurement process involving ultrasonic sensors.

The turbine rotor guide vanes (stator) of a turbofan engine are components which shape the engine gas path. The vanes are also highly exposed to dynamic loads from the hot gas stream (with temperatures ranging from 950 °C to 1650 °C) [11]. Hence, it is essential to improve the high temperature resistance of rotor blades by using ceramic thermal barriers and by cooling the stator during operation. The cooling of the component requires a complex cored casting, where the core forms the internal passageways that transfer the cooling medium and also reduce the component weight. The cooling process results in a temperature gradient across the casting wall section. This temperature gradient induces heavy thermal stresses, which may contribute to failure of the casting (by fracture) and its protective thermal barrier (by chipping, cracking or flaking). The component weight can be reduced, and the stator segment and vane cooling system performance improved, by making the vane casting walls thinner. It is thus critical to assure the dimensional repeatability of wall thickness during the manufacturing process. Among the available NDT (non-destructive test) methods suitable for wall section inspection, e.g. active thermography [12], CT (computer tomography) [13], and eddy current defectoscopy [14], ultrasonic measurement methods [15] are the most popular.

In general, three measurement methods are used during ultrasound measurements: echo [16], shade [17] and resonance [18]. The method selected for the measurement depends on the workpiece size and material. The choice of test medium is also important, and depends on the measurement method used and the environmental conditions. Manual defectoscopy uses gels [19], while robotic or automated systems tend to use water and oils [20, 21]. However, if the measurement temperatures are low, silicone gels are used [22]. In this paper, water was used as the medium.

The need for continuous quality control and the high number of defined measurement points increase the process time, which in turn results in higher costs, and hence leads to the search for automated [20] or robotic solutions [21]. Solutions are also used which include dedicated 2, 3 and 4-axis robots [23] and mobile dedicated robots for special non-destructive testing [24]. In addition to the dedicated robotic structures, there are also a small number of systems based on standard 6-axis robots [25].

This paper presents a developed and implemented robotic inspection station to assess the workmanship quality of rotor castings for jet engine turbines, based on a robot-assisted geometry inspection system.

2 Robot-Assisted Geometry Inspection

The robot-assisted geometry inspection was performed with an ABB IRB 1600 robot manipulator equipped with an ATOS Core 135 optical 3D scanner (Fig. 1) and ATOS Professional control and measurement software suite. With a specific control program developed in ATOS Professional to run the control cabinet commands, the ABB IRB 1600 robot manipulator facilitated all the required positioning and orientation of the optical 3D scanner and automatic measurements [26].

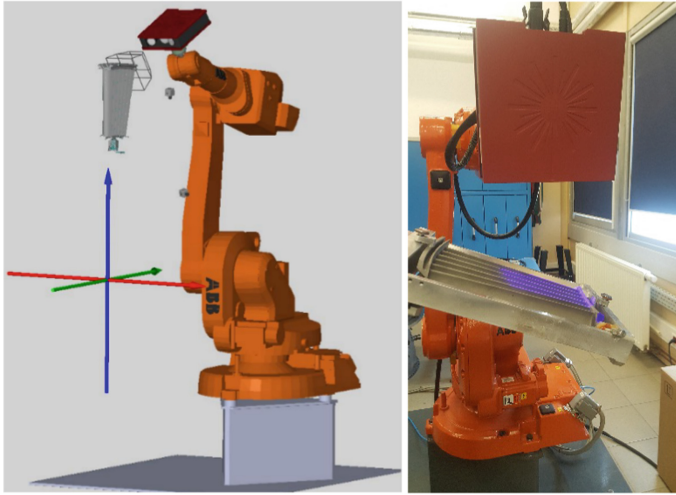


Fig. 1. Virtual and actual geometry inspection stand.

The ATOS Professional software suite can store the spatial measurement positions and orientations of the 3D scanner in order to automate and provide repeatability of successive component inspection runs. When each measurement is complete, the scanner must be moved and rotated to areas not recorded in the preceding scanning run. The individual measurements are automatically processed within a common coordinate system, which produces a complete cloud of 3D points.

The ATOS Core 3D scanner is a triangulated system of stereoscopic cameras (i.e. to calculate the intersection of a specific plane with a beam in three-dimensional space). The scanner projects a system of bands on the inspected surface of the workpiece. The projected bands are recorded by the two stereoscopic cameras (Fig. 2), providing a phase shift image from the sine distribution of intensity on the camera detectors. The ATOS Core uses multiple heterodyne phase shifts to provide the maximum sub-pixel accuracy. Separate 3D coordinates are calculated for each camera detector pixel from optical transformation equations.

This gives a calculated polygonal grid which circumscribes the free surfaces and geometric elements. The polygonal grid is verified by comparing the reproduced

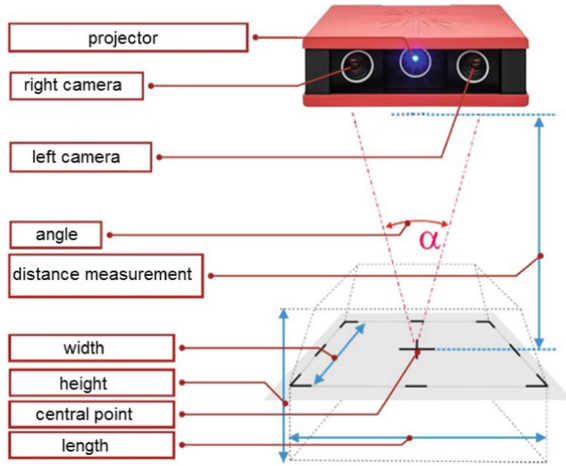


Fig. 2. ATOS Core measurement concept.

surface with the engineering drawing or directly with a set of CAD data [27, 28]. The software can also implement 3D surface analysis and 2D analysis of sections or points.

Each single measurement generates up to 5 million data points. The scanner records only those points visible to both cameras in a single scan. In order to digitize a complete object, several individual measurements are required from different angles. Based on reference points (circular markers), which are attached directly to the object or to the measuring plate or a fixture, Atos transforms these individual measurements automatically into a common global coordinate system.

The Atos Core 135 three-dimensional scanner is equipped with projector and camera lens setups (Table 1).

Table 1. ATOS Core 135 system configurations.

Measuring area	135 × 100 mm
Working distance	170 mm
Point spacing	0.05 mm
Resolution	5 Mpix
Sensor dimensions	206 × 205 × 64 mm
Weight	2.1 kg
Power supply	90–230 V AC
Operating temperature	+ 5 °C up to + 40 °C, non-condensing

There are already several fields where three-dimensional scanning is an established method of data acquisition. In mechanical engineering, 3D scanners are often used for workpiece inspection, deformation analysis, reverse engineering and reengineering of moulds and dies, and general quality control procedures [29, 30]. Civil engineering also

uses three-dimensional scanning during building inspections, custom fit furniture design, and cultural heritage protection and renovations. The textile industry uses scanning for digitalization of the human figure in custom fit product design. The movie industry also widely uses three-dimensional scanning for various CGI effect creation processes. Its use has also spread to the marketing and advertisement industries, [31–34]. This has already caused some degree of specialization by scanner manufacturers regarding the field of use.

The detailed inspection results can be presented in the form of reports, which may include screenshots, measurement charts, diagrams, text and graphic elements. The results can be represented in a graphical format, edited in the user interface or exported as PDF files.

3 Determination of Actual Measurement Point Coordinates

A number of unfavourable phenomena occur during the solidification of the large thin-wall polycrystalline castings of stator segments. These include shrinkage, stress, and ultimately, deformation. Once cleaned, the casting is subject to a preliminary visual inspection. If the casting passes, it is scanned to produce a complete cloud of 3D points with defined parameters (Fig. 3).

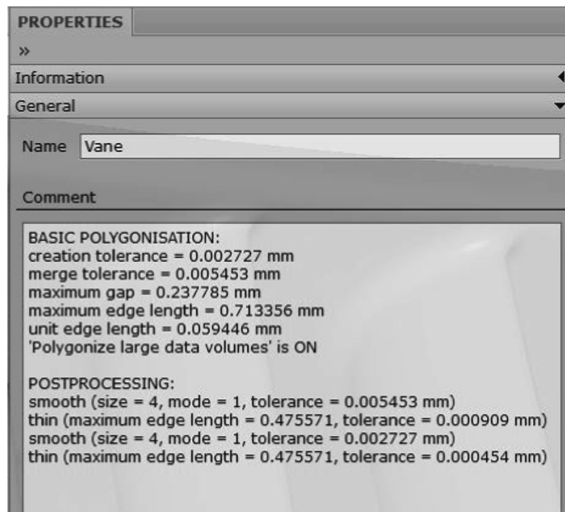


Fig. 3. Parameters of a completed 3D scan.

Atos Professional has an efficient feature called Fast Inspection, which facilitates the display of a colour map showing the deviations from the preset geometric tolerances (Fig. 4) and inspecting the measurement features in real time, directly after each scanning run. The measured results are updated and displayed during the measurement cycle in relation to an imported or manually input measurement plan and a CAD model.

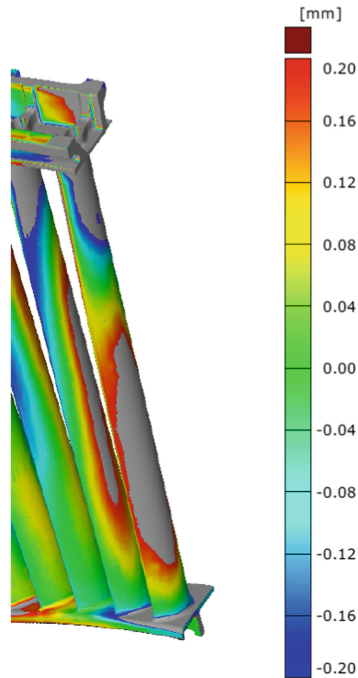


Fig. 4. Colour map of preset geometric tolerance deviations.

The quality control functions for the analysis of airfoils and turbine vanes or blades include checks of: camber line, geometric solid mass centre, turbine blade and vane profile thickness, chords, angle of twist, attack radius, trail radius, etc. For the inspection of castings, a program was developed that generates 42 sections of stator segment vanes, with a comparison of the CAD model with the generated 3D point cloud, the camber line being reproduced at the selected points of the vane section components with geometric tolerance deviations (Fig. 5).

The 3D point cloud fitted to the CAD model as above is used downstream to determine the actual coordinates of the measurement points required to verify the vane wall thickness.

Each of the stator vanes is a precision thin-wall casting and requires the verification of wall thickness at 28 measurement points. The points are determined with utmost precision, and currently the inspection process requires manual marking with a special template. This method has been acceptable so far, since the vane wall thickness has been measured manually, with a hand-held flaw detector. If the section thickness inspection process is conducted with a robot and the UTT method, the points must be input into a controller to manage their locations and measurement. Hence the point coordinates are derived from the 3D scan (the 3D point cloud), generated as described above.

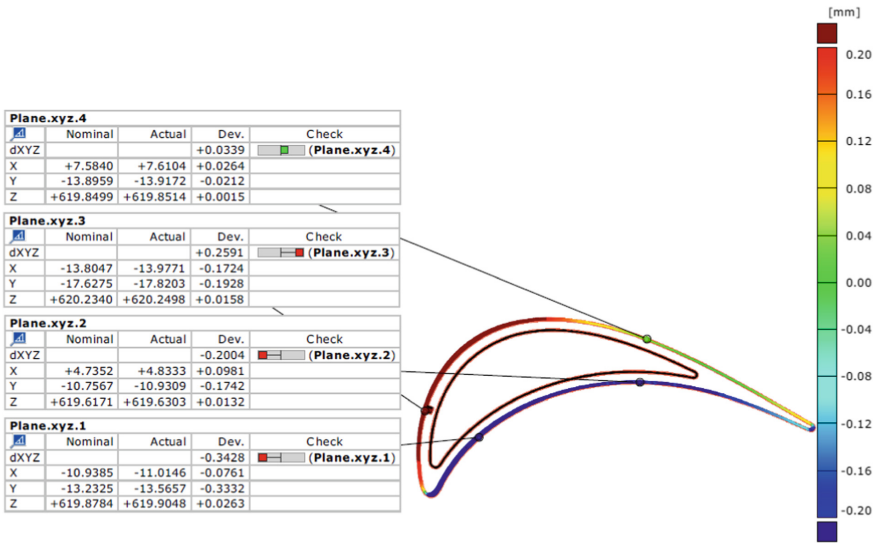


Fig. 5. One of the 42 sections of a stator segment vane.

The nominal workpiece (the CAD model) has the nominal coordinates determined (Fig. 6) for the first 7 points on the vane of the inspected stator, with the actual coordinates for the casting being generated automatically (Fig. 6).

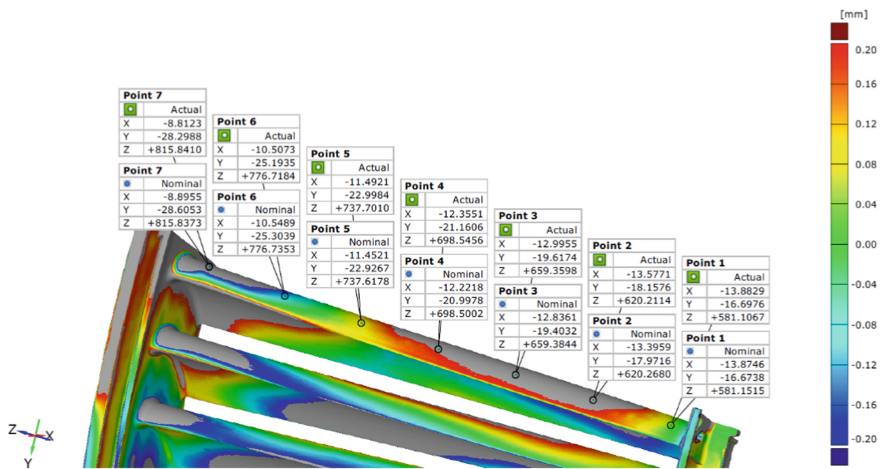


Fig. 6. Nominal and actual measurement points for the generation of motion trajectory applied in the stator vane wall thickness measurement process.

The origin of the coordinate system is selected (offset) during the determination of the actual coordinates of the geometric measurement system (Fig. 1) to match the coordinate system applied to measure vane wall thickness (Fig. 7).



Fig. 7. Robot-assisted vane thickness measurement stand.

4 Robotic Vane Thickness Measurement Stand

The 168 specific coordinates of the actual measurement points, referenced to the nominal points (Fig. 6), are produced for a single complete part of the stator and are input to the controller of the robotic measurement stand (Fig. 7) [35]. The specific coordinates permit the generation of the motion trajectory for the ABB IRB 140 to perform the UTT measurement [36].

The software was designed to assume a robot operating on a fixed object, i.e. the inspected stator, with the robot tools being UT scanning probes (Fig. 8). This assumption was critical to the programming of the solution and greatly facilitated the design process.

The workpiece and its coordinate systems are moved, while both tools are fixed in place. This helps to design the motion paths faster and to modify them with greater ease [37].

The measurement heads (both left and right-hand ones) were permanently fastened and had constant 3D coordinates. The actual measurement point coordinates (Fig. 6) were variable and automatically determined by the robot manipulator with its optical 3D scanner. This rapid determination of the measurement coordinates at 168 points allowed further automatic definition, with a measurement point on the trajectory being defined in each coordinate system, with several waypoints for the approach to the UT scanning probe (Fig. 9b).

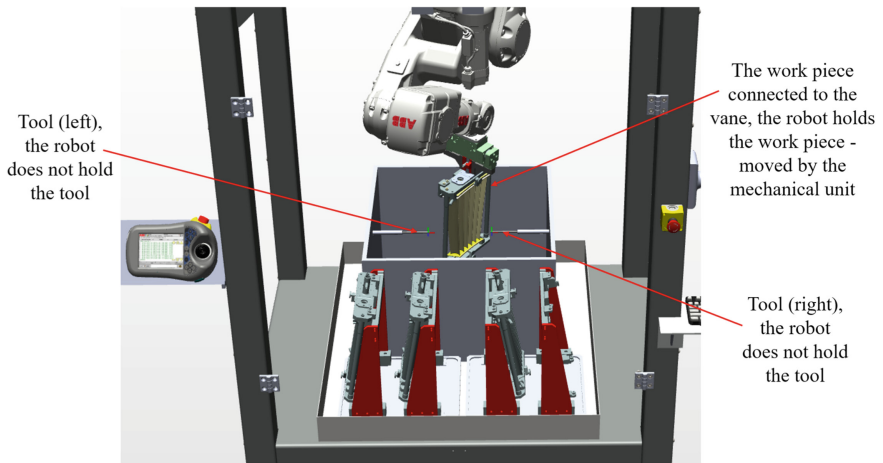


Fig. 8. Layout of the coordinate systems and tools on the test stand.

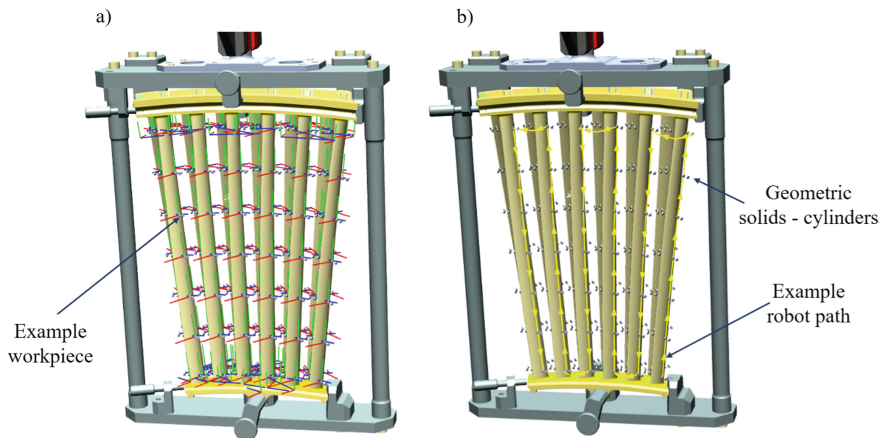


Fig. 9. Measured element: (a) Fixture stator with a stator and defined coordinate systems; (b) Fixture cassette with a stator and an example of the scanning path.

5 UT Measurements of Stator Casting Quality

The application of UT measurements for the determination of material section thickness was based on the physical phenomena of wave propagation, i.e. the reflection (echo) of the wave incident to a medium with physical and chemical characteristics that differ from the tested material. The reflection (echo) point was the interface between the test material and the medium. The phenomenon was caused by the change in the acoustic resistance of the wave. The reflected wave amplitude increased with increases in wave resistance difference between the two media. Therefore, if an echo of the sound wave was present in the investigated medium, there must have been a discontinuity

within the medium. If the time from transmitting the sound wave in the tested medium to the return of the wave reflected by that discontinuity was measurable, and the wave propagation velocity in the given material was known, then the distance covered by the wave was calculable and hence the material thickness could be determined.

The produced robotic test station application used a UT wave transceiver formed by two piezoelectric elements. The location of the piezoelectric elements was determined by the form of the inspected casting. The location of the piezoelectric transceivers was determined by simulation in RobotStudio.

The robotic measurement of vane wall thickness involved the verification of the casting section thickness along a sequence of measurement points. The couplant used was water. An example of the measurement signal is shown in Fig. 10. The visualised wave trend featured three characteristic areas. Area 1 was the wave echo caused by the design of the UT probe. This trend fragment had no relevant measurement data. Area 2 was the echo at the interface between the couplant and the outer casting surface. Area 3 was the echo at the interface between the casting and the couplant.

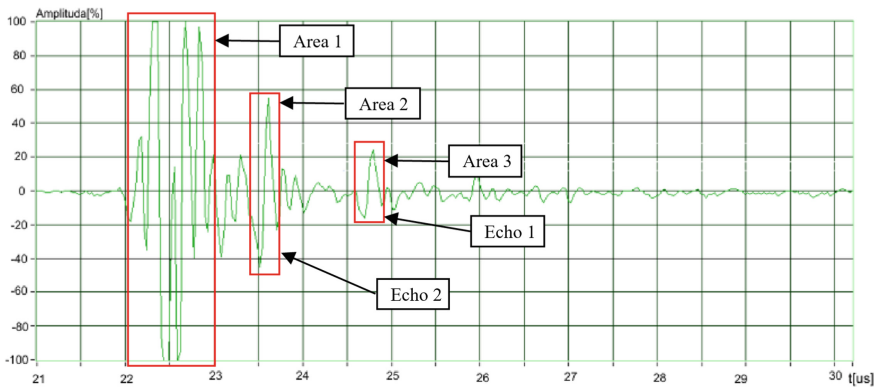


Fig. 10. Example measurement signal showing characteristic areas.

The thickness was measured with upper signal amplitudes, which eliminated the measurement of the distance between the upper and lower halves of the amplitude. The measurement was performed by determining the time of signal transition between echo 1 and echo 2. Three level indicators, or gates (Fig. 11), were used in this measurement. Gate 1 was the detection of the echo maximum and it automatically determined the signal analysis area on the x-axis. Based on the gate 1 position value, the coordinate x value of gate 2 was dynamically determined. This facilitated locating the echo 1 amplitude value (Fig. 1) within gate 2. In the next step, the gate 2 value was used to automatically determine the coordinate x value of gate 3. This facilitated locating the echo 2 amplitude value (Fig. 1) within gate 3. Thanks to the dynamic gate positioning, the measurement system was immune to the effects of changes in the distance of the UT transceiver probe from the test item.

The coordinate y values of gates 1 and 2 were selected experimentally to have echo values higher than the values assumed for the gate level. The lower limit must be higher

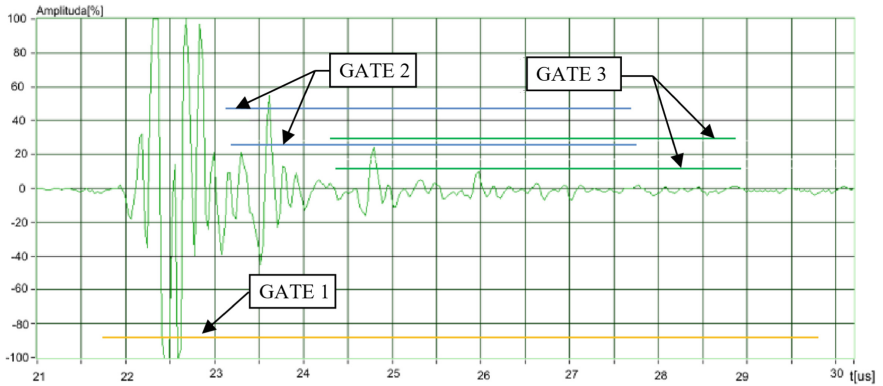


Fig. 11. Example of the measurement signal with characteristic areas.

than the signal variation amplitude. During the experiments, the y value was 20% of the maximum signal amplitude.

The applied measurement method required calibrating the UT wave propagation velocity for the test item material. The calibration process for the test stand discussed here was automatic: when a standard item thickness was input, the calibration function automatically determined the coefficient of wave propagation velocity.

The software suite of the test stand featured an advanced UT defectoscope functionality and digital connectivity with the robot controller. The application level allowed management of the UT signal parameters. The software was able to store the recorded measurement results as a HTML report and the settings as an INI file.

The software allowed adjustment of the UT transceiver probe output pulse frequency, the pulse generation repeat interval, and the pulse generation voltage. The

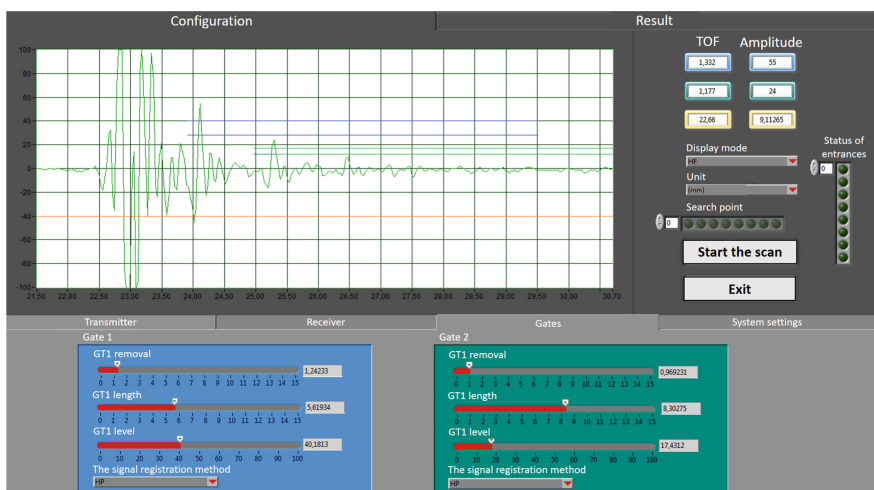


Fig. 12. Measurement software: user panel view.

software also permitted selection of: analysed signal range, signal recording start delay, signal gain (dB) value, frequency band, signal attenuation, and signal averaging method. Figure 12 shows an example of the ImageSonic software user panel.

An example of the measurement report (Fig. 13) was generated as a HTML file at the end of the measurement. The output measurement report featured test item iden-

	Blade 1	Blade 2	Blade 3	Blade 4	Blade 5	Blade 6	Mean	Deviation	Minimum	Maksimum
1	0,68145	1,6107	0,92925	0,8673	1,42485	1,06864	1,09703	0,353769	1,6107	0,68145
2	0,712425	0,665963	0,68145	0,68145	0,665963	0,68145	0,68145	0,0169657	0,712425	0,665963
3	1,03766	0,727912	1,54875	0,712425	0,80535	0,68145	0,918925	0,334425	1,54875	0,68145
4	1,40936	0,92925	0,665963	0,7434	0,92925	1,70363	1,06347	0,40643	1,70363	0,665963
5	1,37839	1,51777	0,665963	1,4868	1,54875	0,68145	1,21319	0,421837	1,54875	0,665963
6	0,712425	1,17705	0,68145	1,31644	0,898275	0,882787	0,944738	0,253541	1,31644	0,68145
7	0,9912	0,898275	0,7434	0,712425	1,13059	0,712425	0,864719	0,172577	1,13059	0,712425

Fig. 13. Example measurement report.

tification, thickness values at individual measurement points on the vanes, and statistical data (mean, deviation, minimum and maximum values per data line).

6 Conclusion

This paper presents a robotic geometry inspection stand equipped with a scanner device, a GOM software suite and an ABB robot. The paper discusses a method of automatic geometry scanning, and the results produced by that process are compared with a measurement model (nominal) to perform an initial geometry verification of the casting and determine 168 specific coordinates for the actual measurement points that are necessary to generate the motion trajectory for the other robotic test stand, used for the UTT measurement of the precision thin-wall casting of the vanes. The correctness of the solution has been proved with scans and measurements of two turbine rotor guide vane segments of an aircraft engine provided by courtesy of Consolidated Precision Products Poland sp. z o.o. The maximum correction of the measurement point coordinates for the two stator segments was approximately 0.4 mm. The paper presents a robotic test stand for UTT quality control. The design and fabrication process of the test stand was not discussed here. The operating principle of its measurement system is presented, with a specific focus on the measurement strategy. Following a verification of the presented solutions, the measurement time per single stator was reduced from 6 h to 15 min. With the future development of optical scanning systems and the increasing accuracy of scanned data, the use of this system will undoubtedly widen to include other areas of inspection, as an alternative to conventional measurement methods.

References

1. Gierlak, P., Burghardt, A., Szybicki, D., Szuster, M., Muszyńska, M.: On-line manipulator tool condition monitoring based on vibration analysis. *Mech. Syst. Signal Process.* **89**, 14–26 (2017)
2. Giergiel, J., Kurc, K.: Identification of the mathematical model of an inspection mobile robot with fuzzy logic systems and neural networks. *J. Theor. Appl. Mech.* **49**, 209–225 (2011)
3. Tutak, J.S.: Virtual reality and exercises for paretic upper limb of stroke survivors. *Tehnički vjesnik* **24** (Supplement 2), 451–458 (2017)
4. Kurc, K., Szybicki, D., Burghardt, A., Muszyńska, M.: The application of virtual prototyping methods to determine the dynamic parameters of mobile robot. *Open Eng.* **6** (1), 55–63 (2016)
5. Tutak, J.S.: Design of ELISE robot for the paretic upper limb of stroke survivors. *J. Vibroengineering* **18**(6), 4069–4085 (2016)
6. Kohut, P., Kurc, K., Szybicki, D., Cioch, W., Burdzik, R.: 1823. Vision-based motion analysis and deflection measurement of a robot's crawler unit. *J. Vibroengineering* **17**(8), 4112–4121 (2015)
7. Kohut, P., Holak, K., Dworakowski, Z., Mendrok, K.: Vision-based measurement systems for static and dynamic characteristics of overhead lines. *J. Vibroengineering* **18**(4), 2113–2122 (2016)
8. Trojnecki, M., Dąbek, P.: Determination of motion parameters with inertial measurement units—Part 2: algorithm verification with a four-wheeled mobile robot and low-cost MEMS sensors. In: *Mechatronics-Ideas for Industrial Application*, pp. 253–267. Springer, Cham (2015)
9. Kohut, P., Holak, K., Martowicz, A.: An uncertainty propagation in developed vision based measurement system aided by numerical and experimental tests. *J. Theor. Appl. Mech.* **50** (4), 1049–1061 (2012)
10. Burghardt, A., Szybicki, D., Kurc, K., Muszyńska, M., Mucha, J.: Experimental Study of Inconel 718 surface treatment by edge robotic Deburring with force control. *Strength Mater.* **49**(4), 594–604 (2017)
11. Sieniawski, J.: Nickel and titanium alloys in aircraft turbine engines. *Adv. Manuf. Sci. Technol.* **27**(3), 23–33 (2003)
12. Carl, V., Becker, E., Sperling, A.: Thermography inspection system for gas turbine blades. In: *7th European Conference on non-destructive testing*, pp. 2658–2665. Copenhagen (1998)
13. Kilian, D.: 3D tomography of turbine blades. In: *Proceedings of the International Symposium of Computerized Tomography for Industrial Applications*, vol. 31, pp. 1–17. Berlin (1999)
14. Le Bihan, Y., Joubert, P.Y., Placko, D.: Wall thickness evaluation of single-crystal hollow blades by eddy current sensor. *NDT E Int.* **34**(5), 363–368 (2001)
15. Lane, C.: The development of a 2D ultrasonic array inspection for single crystal turbine blades. Springer Theses. pp. 63–79. Springer International Publishing, Switzerland (2014)
16. Krause, M., et al.: Comparison of pulse-echo methods for testing concrete. *NDT E Int.* **30**(4), 195–204 (1997)
17. Chakroun, N., Fink, M.A., Wu, F.: Time reversal processing in ultrasonic nondestructive testing. *IEEE Trans. Ultrasonics Ferroelectrics Freq. Control* **42**(6), 1087–1098 (1995)
18. Schindel, D.W., Hutchins, D.A., Grandia, W.A.: Capacitive and piezoelectric air-coupled transducers for resonant ultrasonic inspection. *Ultrasonics* **34**(6), 621–627 (1996)

19. Garnier, C., Pastor, M.L., Eyma, F., Lorrain, B.: The detection of aeronautical defects in situ on composite structures using non destructive testing. *Compos. Struct.* **93**(5), 1328–1336 (2011)
20. D'orazio, T., Leo, M., Distante, A., Guaragnella, C., Pianese, V., Cavaccini, G.: Automatic ultrasonic inspection for internal defect detection in composite materials. *NDT e Int.* **41**(2), 145–154 (2008)
21. Tanase, L., Margaritescu, M.: Quality control of product/process using nondestructive control and possibilities of robotic investigation. In: SIOEL'99: Sixth Symposium on Optoelectronics, vol. 4068, pp. 364–375. International Society for Optics and Photonics (2000, February)
22. Yao, Y., Liu, S., Zhang, W.: Regeneration of silica gel using high-intensity ultrasonic under low temperatures. *Energy Fuels* **23**(1), 457–463 (2008)
23. Steiner, K.V.: Defect classifications in composites using ultrasonic nondestructive evaluation techniques. In: *Damage Detection in Composite Materials*. ASTM International (1992)
24. Kersting, T., Schönartz, N., Oesterlein, L., Liessem, A.: High end inspection by filmless radiography on LSAW large diameter pipes. *NDT E Int.* **43**(3), 206–209 (2010)
25. Mineo, C., Pierce, S.G., Nicholson, P.I., Cooper, I.: Robotic path planning for non-destructive testing—A custom MATLAB toolbox approach. *Robot. Comput. Integr. Manuf.* **37**, 1–12 (2016)
26. Burghardt, A., Kurc, K., Szybicki, D., Muszyńska, M., Szczęch, T.: Robot-operated inspection of aircraft engine turbine rotor guide vane segment geometry. *Tehnicki Vjesnik-Technical Gazette* **24**(Supplement 2), 345–348 (2017)
27. Liu, B., et al.: Virtual plate pre-bending for the long bone fracture based on axis pre-alignment. *Comput. Med. Imaging Gr.* **38**(4), 233–244 (2014)
28. Lavoué, G., Tola, M., Dupont, F., Lavou, G.: MEPP-3D mesh processing platform. In: *GRAPP/IVAPP*, 206–210 (2012)
29. Brajljih, T., et al.: Possibilities of using three-dimensional optical scanning in complex geometrical inspection. *Strojniški vestnik-Journal of Mechanical Engineering* **57**(11), 826–833 (2011)
30. GOM. Quality control of injection moulded parts, from <http://www.gom.com/EN/BOC.html>. Accessed 31 May 2009
31. Dúbravčík, M., Kender, Š.: Application of reverse engineering techniques in mechanics system services. *Proced. Eng.* **48**, 96–104 (2012)
32. Paulic, M., Irgolic, T., Balic, J., Cus, F., Cupar, A., Brajljih, T., Drstvensek, I.: Reverse engineering of parts with optical scanning and additive manufacturing. *Proced. Eng.* **69**, 795–803 (2014)
33. Pogacar, V.: Integrated renaissance of design. In: *Proceedings of the 1st DAAAM International specialized conference on additive technologies*, pp. 9–12. Celje (2007)
34. Min, Z.H.O.U.: A new approach of composite surface reconstruction based on reverse engineering. *Proced. Eng.* **23**, 594–599 (2011)
35. Burghardt, A., Kurc, K., Szybicki, D., Muszyńska, M., Szczęch, T.: Monitoring the parameters of the robot-operated quality control process. *Adv. Sci. Technol. Res. J.* **11**(1), 232–236 (2017)
36. Burghardt, A., Kurc, K., Szybicki, D., Muszyńska, M., Nawrocki, J.: Robot-operated quality control station based on the UTT method. *Open Eng.* **7**(1), 37–42 (2017)
37. Burghardt, A., Kurc, K., Szybicki, D., Muszyńska, M., Nawrocki, J.: Software for the robot-operated inspection station for engine guide vanes taking into consideration the geometric variability of parts. *Tehnicki Vjesnik-Technical Gazette* **24**(Supplement 2), 349–353 (2017)